Optimising a non-tubular adhesive bonded joint for uniform torsional strength

Nicola Pugno

Dept. of Structural Engineering, Politecnico di Torino, Corso Duca degli Abruzzi 24, 10129 Torino, Italy

Abstract: The paper analyses the problem of optimising the profile of a non-tubular adhesive bonded lap joint under torsion. The joint considered consists of two thin rectangular section beams bonded together along a side surface. The aim of the investigation is to make the joint uniformly resistant to torsion, without however weakening it in other stress situations: the result is a stronger and lighter structural element.

The predominant stress field developed in the adhesive at the bond area between the two beams in *single-lap* and *scarf* joints is determined. The stress field pattern is highly nonlinear along the longitudinal coordinate (joint axis) and is heavily dependent on joint geometry: maximum stresses are reached at the ends of the adhesive for the first type of joint, and along its centerline for the second type.

An intermediate type of joint can be produced by modifying the joint profile, thus ensuring that the stress field is constant along the longitudinal coordinate and thereby optimising the joint for uniform torsional strength.

Keywords: bonded joint, non-tubular, optimisation, torsion.

Reference to this article should be made as follows: Pugno, N. (1999) 'Optimising a non-tubular adhesive bonded joint for uniform torsional strength,' *Int. J. of Materials and Product Technology*, Vol. 14, Nos. 5/6, pp. 476-487.

Introduction

The use of light alloys and composite materials is spreading in automotive and mechanical applications, as well as in aircraft construction. In addition, the development of epoxy resin-based adhesives has brought a wide range of advantages, as such adhesives make it possible to reduce structural weight, prevent the onset of corrosion, achieve better stress distribution in the adhesive layer, join dissimilar materials (e.g. steel and composites), and produce smooth surface contours, a major benefit for components exposed to a fluid current. All of these advantages encourage the designer to consider adhesive bonding for structures which until recently were joined using conventional techniques such as riveting, welding or threaded connections.

The drawbacks associated with adhesives in the past, including their limited service temperature range and susceptibility to chemical attack, have to a large extent been overcome.

As the literature indicates, studies have hitherto concentrated on the effects of axial force, flexure and shear on adhesive bonded joints. In certain situations, however, such joints are also subject to torsion. Research in this area is restricted to tubular structures [1-31], as other cases are entirely lacking in the literature. A detailed bibliography of the literature on adhesive bonded joints under torsion is given in this paper. The lack of work on non-tubular joints indicated by this bibliography motivated the investigation presented in [32], which was used as the basis for [33-35] as well as for this paper.

This gap in the literature can perhaps be explained by noting that non-tubular adhesive bonded joints are not designed to withstand a torsional moment, which can thus induce a non-shearing stress state in the adhesive of such joints. As is well known, in fact, adhesive is by nature less effective when subjected to normal stresses (as is illustrated by the differences encountered when attempting to separate two pieces of adhesive tape by applying tensile or shear stresses). Though this is likely to be the major reason that little work has been done with non-tubular joints, it cannot be considered a justification. During its service life, in fact, a non-tubular adhesive bonded joint can find itself called upon to withstand accidental torsional loading: as the joint is not designed for this type of characteristic of internal reaction, even modest torsional loads can prove to be critical.

From these considerations, it is clearly important to optimise the joint for torsion, precisely because of its marked sensitivity to this characteristic of internal reaction. Starting from the *single-lap* configuration, optimisation was achieved by chamfering the edges, which are in any case not involved in the stress flow induced by the tensile loading for which the joint should be designed. The resulting optimised joint is thus both lighter and stronger.

Torsional moment transmission and predominant stress field in the adhesive

It is assumed that the materials making up the joint (Figure 1) are governed by a linear elastic law. While this is intuitively obvious for the beams (which are typically metal), this is not the case for the adhesive, which is more likely to show a typically nonlinear elastic behaviour.

Under torsion, however, the stress state in the adhesive relative to a non-tubular bonded joint is basically normal. As it is well known that adhesive can withstand shearing stresses which are an order of magnitude higher than the ultimate normal stresses, it follows that the normal stresses occurring in the adhesive during service must be limited. It is precisely because of these modest stresses that we can assume that the adhesive is also governed by a linear elastic law.

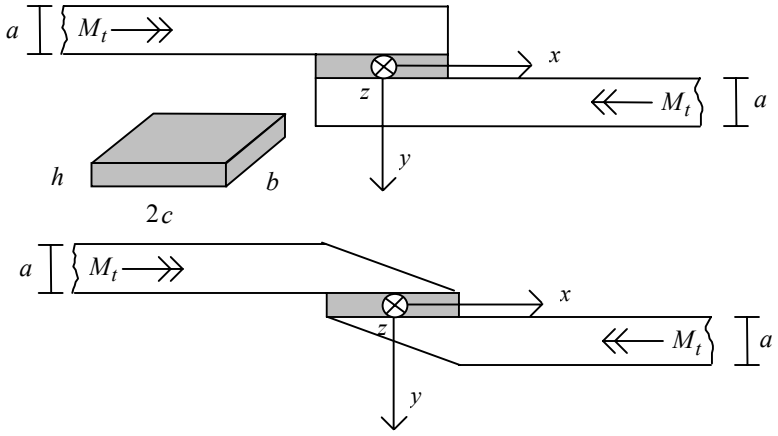

Figure 1 *The two different types of conventional joint analyzed: single-lap (top) and scarf (bottom)*

Assuming linear elastic laws and using equilibrium and compatibility equations to solve the torsional problem, the function which governs transmission of the torsional moment along the overlap, or in other words, how the torsional moment progresses section by section along the top beam, can be found by solving the following differential equation [32,33,35]:

$$\frac{d^2M(x)}{dx^2}+C\frac{I_{t_1}(x)+I_{t_2}(x)}{I_{t_1}(x)I_{t_2}(x)}M(x)=-\frac{CM_t}{I_{t_2}(x)} \quad \begin{cases} M(x=-c)=M_t \\ M(x=c)=0 \end{cases} \tag{1}$$

where x is the longitudinal coordinate of the joint (Figure 1).

The torsional moment on the top beam found section by section in the thin adhesive layer is designated as M, while C is a constant which is a function of the joint's construction and geometrical characteristics (Table 1: $M=M_1$, $C=K^*/G$). I_t is the factor of torsional rigidity which, in the case of the thin rectangular section considered here, can be expressed by the following relation:

$$\begin{aligned} &I_{t_{1,2}}=\frac{b}{3}a^3 \quad single-lap \\ &I_{t_{1,2}}(x)=\frac{b}{3}\left[\frac{a}{2}\left(1\mp\frac{x}{c}\right)\right]^3 \quad scarf \end{aligned} \tag{2}$$

The equations above indicate that the solution to the problem (Equation (1)) is heavily dependent on joint geometry (Equation (2)).

At this point, the predominant stress field in the adhesive (equivalent to the applied torsional moment) can be determined by imposing rotational equilibrium of an infinitesimal beam element belonging to the bond area [32,33,35]:

$$\sigma_y(x,z)=-\frac{z}{I_x^*}\frac{dM(x)}{dx} \tag{3}$$

Table 1 Analytical relations governing torsional moments in the two beams and the corresponding predominant stress fields for single-lap and scarf joints

Notation

a: Height of beam cross section

b: Width of cross section through the beam and bond

c: Half length of bond

h: Height of bond

G: Shear elastic modulus of beam material

E_a:: Normal elastic modulus of adhesive material

ν_a: Ratio of transverse contraction of adhesive material

Constants

$$I_x^* = \frac{b^3}{12},\ E_a^* = \frac{1-\nu_a}{(1+\nu_a)(1-2\nu_a)}E_a,\ K^* = \frac{E_a^* I_x^*}{h},\ A = \sqrt{\frac{6K^*}{Ga^3 b}},\ H = \frac{Ga^3 b}{24K^* c^2}$$

Torsional Moments

$$M_1(x) = M_t f(x)$$

$$M_2(x) = M_t(1 - f(x))$$

Stress Field

$$\sigma_y(x,z) = -\frac{M_t}{I_x^*} z \frac{df(x)}{dx}$$

Single-lap

$$f(x) = \frac{1}{2}\left(1 - \frac{\sinh(Ax)}{\sinh(Ac)}\right)$$

Scarf

$$f(x) = \frac{1}{2} + \sum_{n=1}^{\infty} l_{2n-1}\left(\frac{x}{c}\right)^{2n-1},\ l_{2n-1} = c_{2n-1} + d_{2n-1}a_1,\ l_1 = -\frac{\frac{1}{2} + \sum_{n=1}^{\infty} c_{2n-1}}{\sum_{n=1}^{\infty} d_{2n-1}}$$

$$\begin{cases} c_1 = 0 \\ d_1 = 1 \end{cases} \quad \begin{cases} c_3 = \frac{1}{2H} \\ d_3 = \frac{1}{3H} \end{cases} \quad \begin{cases} c_5 = \frac{10H+1}{20H^2} \\ d_5 = \frac{18H+1}{30H^2} \end{cases} \quad \begin{cases} c_7 = \frac{210H^2+70H+1}{420H^3} \\ d_7 = \frac{450H^2+78H+1}{630H^3} \end{cases}$$

$$(c,d)_{2n+1} = \frac{\frac{2}{H} + 3(2n-1)(2n-2)}{(2n+1)(2n)}(c,d)_{2n-1} + \frac{\frac{6}{H} - 3(2n-3)(2n-4)}{(2n+1)(2n)} \cdot$$

$$\cdot (c,d)_{2n-3} + \frac{(2n-5)(2n-6)}{(2n+1)(2n)}(c,d)_{2n-5} \quad \forall n \geq 4$$

In Equation (3) I_x^* is a moment of inertia per unit length (Table 1) and z is the transverse coordinate (Figure 1). Equation (3) demonstrates that the increase in torsional moment occurring at the ends of the infinitesimal element considered is balanced by the normal stresses that the adhesive exerts on the beam.

Following a three dimensional finite element analysis, the mathematical approach was validated by comparing the predominant stress field given by relation (3) with that determined numerically, indicating an error on the stress peak of less than 4% [32,35].

Analytical results are given in Table 1. A torsional moment transfer function $f(x)$ is introduced which reproduces M, amplified by the applied external torsional moment. As indicated by relation (3), its derivative multiplied by the transverse coordinate z governs the predominant stress field in the adhesive.

Figures 2 and 3 show qualitative curves for the torsional moment section by section along the lap joint, while the predominant stress field in the adhesive is presented in Figures 4 and 5.

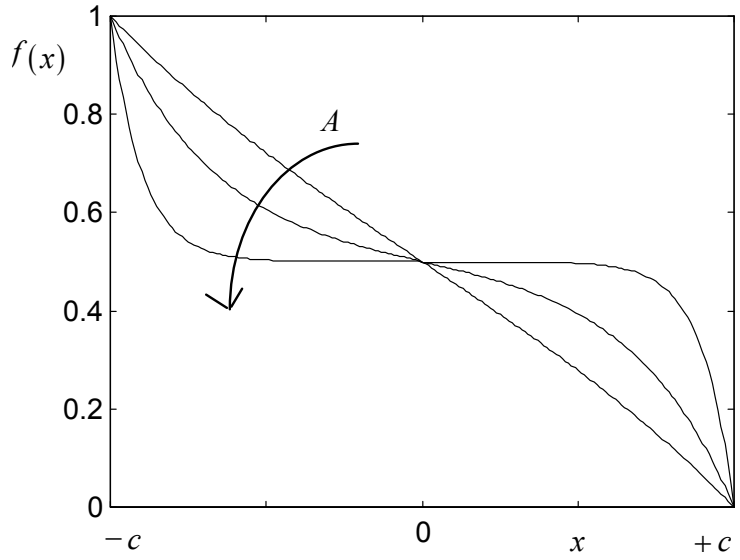

Figure 2 *Curve for function* $f(x)$ *which reproduces the torsional moment along the bond, amplified using a given constant, for the single-lap joint*

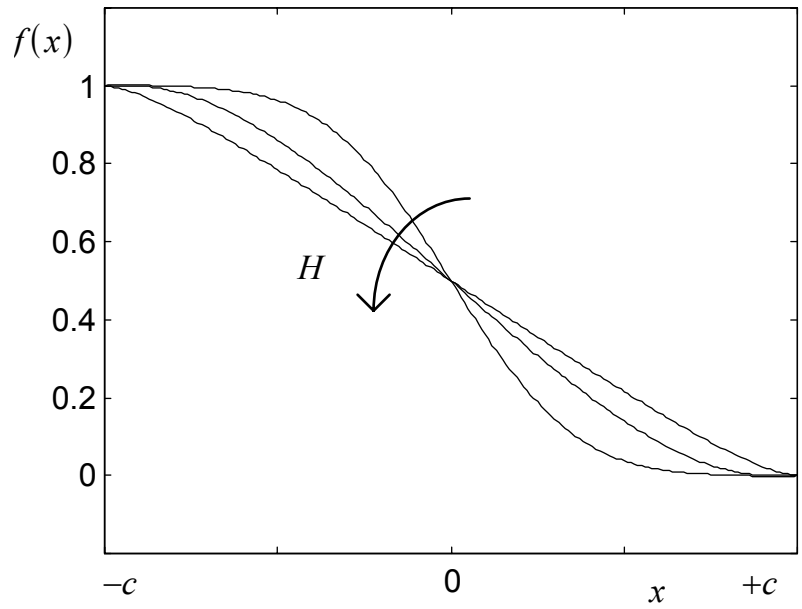

Figure 3 *Curve for function* $f(x)$ *which reproduces the torsional moment along the bond, amplified using a given constant, for the scarf joint*

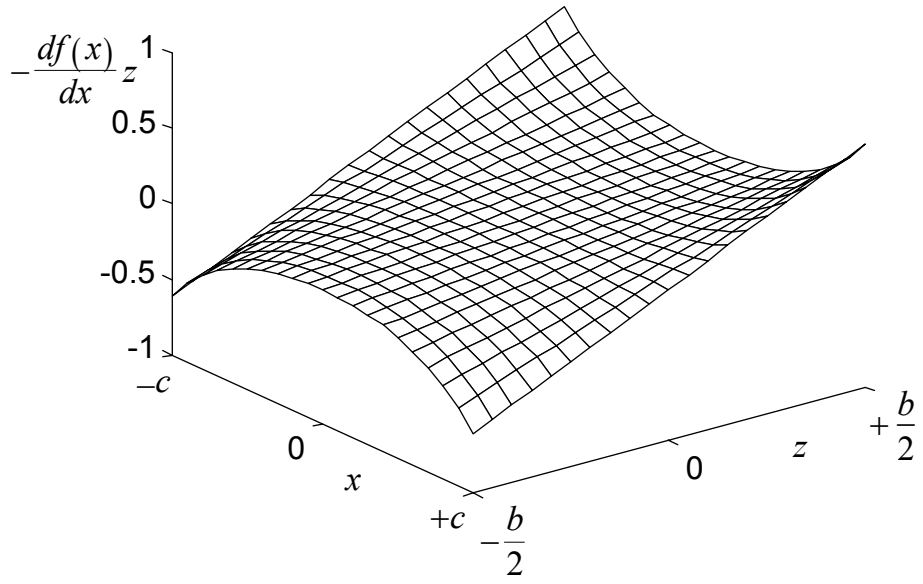

Figure 4 *Surface for function* $-\frac{df(x)}{dx}z$ *which reproduces the predominant stress field in the adhesive, amplified using a given constant, for the single-lap joint*

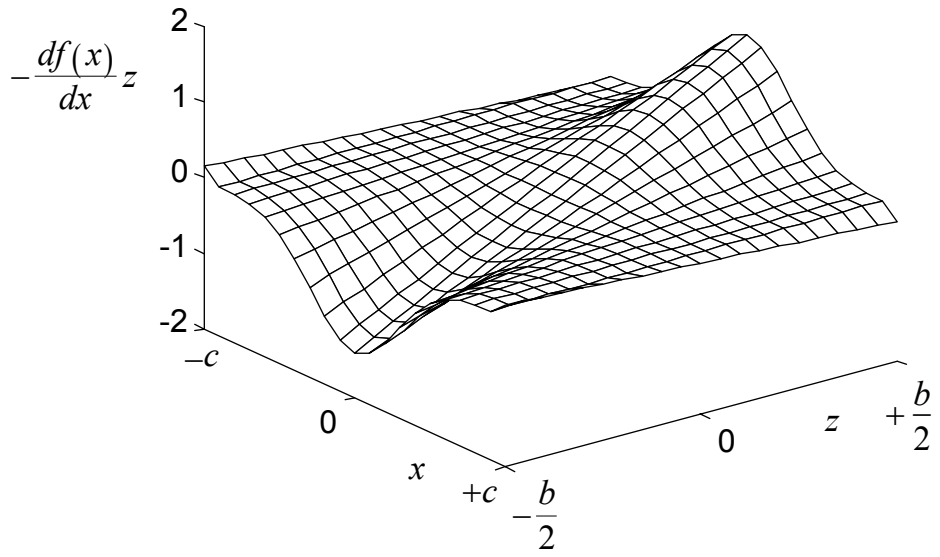

Figure 5 *Surface for function* $-\frac{df(x)}{dx}z$ *which reproduces the predominant stress field in the adhesive, amplified using a given constant, for the scarf joint*

While the stress field distribution shown in Figure 4 is more conventional, as it presents the characteristic stress peaks at the ends of the bond area, the surface in Figure 5 is unusual. However, it can be explained by noting that the torsional moment absorbed by the two beams is proportionate to the corresponding torsional stiffness (which in turn is proportionate to the cube of the height). In any given section of the overlap, the top beam in the *scarf* joint will thus tend to absorb almost all of the transmitted torsional moment, whose maximum variation will consequently take place at the centerline of the joint. The variation in torsional moment is balanced by the stresses that the adhesive transmits to the beam. By contrast with the situation for *single-lap* joints, these stresses will thus also be highest at the centerline.

As expected, this indicates that the stress field is extremely sensitive to external geometry.

Optimising the joint for uniform strength

In observing the geometries and stress field curves for *single-lap* and *scarf* joints (Figure 6), the advantages of finding an intermediate profile for leveling the stress field along the x coordinate are immediately apparent. The dependence along the z coordinate cannot be eliminated, as the predominant stress field must obviously be equivalent to the applied torsional moment.

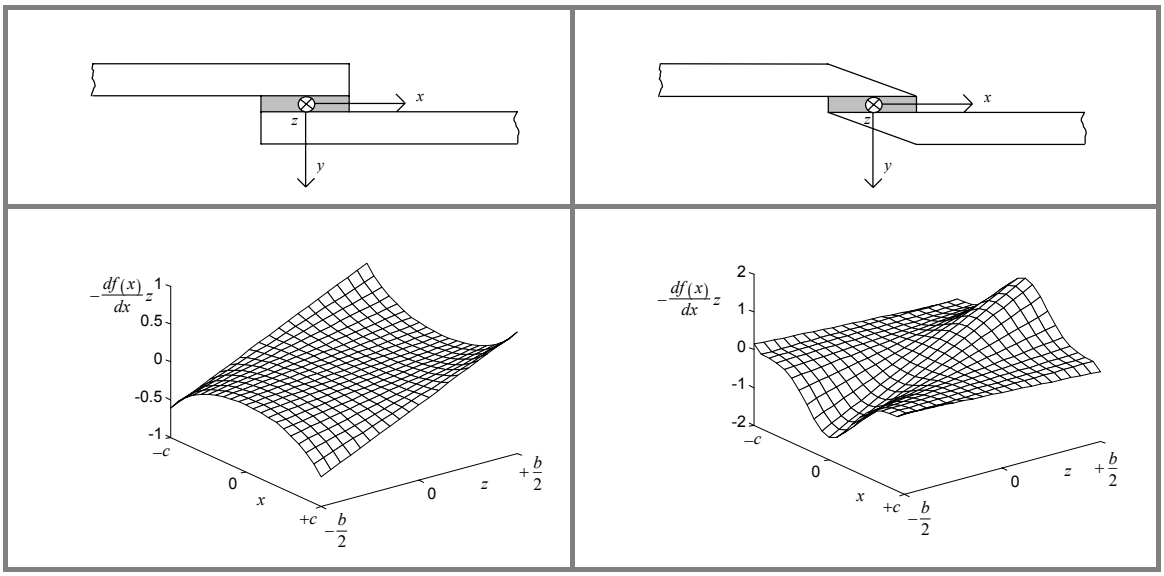

Figure 6 *Comparison of geometries and predominant stress fields for single-lap and scarf joints*

The procedure used is a reversal of that employed for a joint of known geometry: rather than starting from the geometry in order to determine the stress field, the procedure starts with the stress field and finds the geometry capable of ensuring it.

In order to make the stress field constant (in a plane at z = const.), it must be independent of the x coordinate. In other words, as shown by relation (3), the torsional moment must be linear along the joint x axis:

$$M(x) = \frac{M_t}{2}\left(1 - \frac{x}{c}\right) \tag{4}$$

Inserting Equation (4) in (1) yields the following relation, which defines the geometry of a uniform torsional strength adhesive bonded joint:

$$\frac{I_{t_2}(x)}{I_{t_1}(x)} = \frac{c + x}{c - x} \tag{5}$$

The factor of torsional rigidity for a thin rectangular section beam of base b and height $a_i(x)$ can be expressed as:

$$I_{t_i}(x) = \frac{1}{3} b a_i{}^3(x) \tag{6}$$

and Equation (5) is particularised in the following relation:

$$\frac{a_2^3(x)}{a_1^3(x)} = \frac{c + x}{c - x} \tag{7}$$

From the foregoing relation (7), we see that the height of the terminal portion of the beams must be zero; in fact:

$$a_1(x = c) = 0 \quad a_2(x = -c) = 0 \tag{8}$$

In order to identify families of optimised bonded joint profiles, it is necessary to introduce a function of some kind, $a_1(x)$ for example, which respects the previous condition (8). Then, through relation (7), we determine the function $a_2(x)$ whereby the joint has uniform torsional strength.

Though the number of possible geometries which satisfy the relations indicated above is infinite, the following additional condition must be taken into account in order to consider the solution entailing beams with identical profiles:

$$a_1(x) = a_2(-x) \tag{9}$$

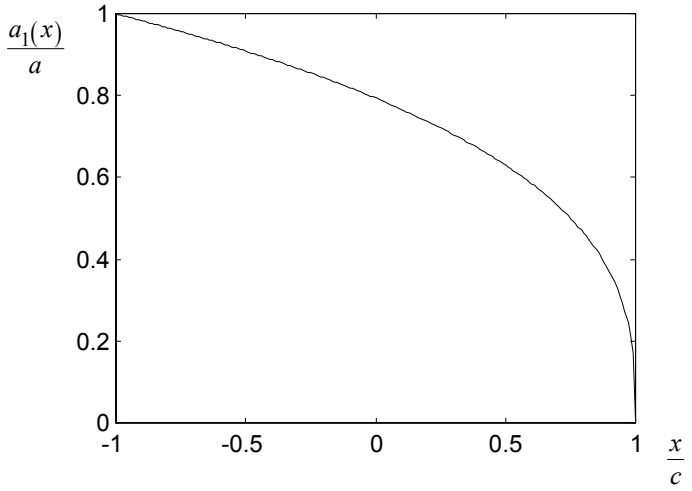

Figure 7 *Beam profile height in the joint optimised for uniform torsional strength (uts)*

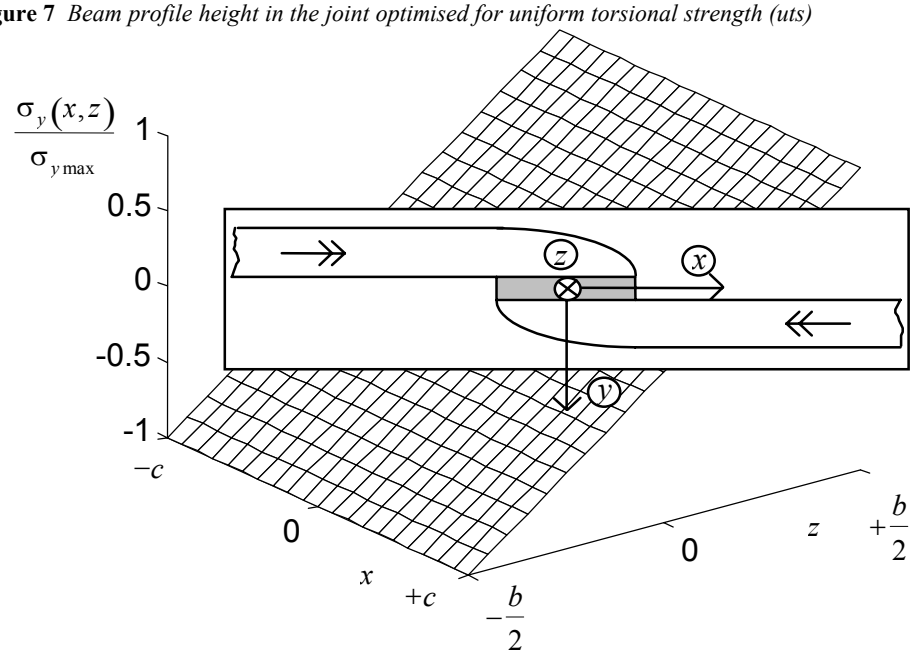

Figure 8 *Geometry of the joint optimised for uniform torsional strength (uts) and the corresponding predominant stress field*

Relations (7) and (9) are satisfied by the following expressions for the profiles of the two beams which define the geometry of the joint optimised for uniform torsional strength (*uts*) and consisting of identical beams:

$$a_1(x)=\sqrt[3]{\frac{c-x}{2c}}a, \quad a_2(x)=\sqrt[3]{\frac{c+x}{2c}}a \tag{10}$$

The profile thus obtained (10) is shown in Figure 7.

The predominant stress field in the adhesive between two beams having the profile described by (10) is thus leveled, as is represented in Figure 8.

Gain of uniform strength joints

In the light of the formulas given above (Table 1), we can define a stress peak parameter which indicates the extent to which the maximum stress departs from the mean. The maximum stress for the two non-optimised joint types considered will be:

$$\begin{aligned}\sigma_{y_{\max}} &= \sigma_y\left(x=c, z=\frac{b}{2}\right)=\frac{M_t}{I_x^*}\frac{Ab}{4}\operatorname{ctanh}(Ac) \quad single-lap \\ \sigma_{y_{\max}} &= \sigma_y\left(x=0, z=\frac{b}{2}\right)=-\frac{M_t}{I_x^*}\frac{b}{2c}l_1 \qquad scarf\end{aligned} \tag{11}$$

while their mean value (on the critical plane $z=b/2$) is:

$$\sigma_{y_{\text{med}}}=\frac{1}{2c}\int_{-c}^{+c}\sigma_y\left(x, z=\frac{b}{2}\right)dx=\frac{M_t}{I_x^*}\frac{b}{4c} \tag{12}$$

Consequently, the peak parameter can be expressed as:

$$\lambda_{\substack{single-lap\\scarf}}=\frac{\sigma_{y_{\max}}}{\sigma_{y_{\text{med}}}}=\begin{cases}\operatorname{ctanh}(Ac)Ac & single\text{ - }lap\\ -2l_1 & scarf\end{cases} \tag{13}$$

As the bond half length of a *single-lap* joint tends to infinity, the maximum stress tends asymptotically to a minimum nonzero value. From a certain point onwards, an increase in the bond half length leads to a reduction in the maximum stress which is insignificant from an engineering standpoint. This does not occur for *uts* joints, where the maximum stress coincides with the mean value expressed by (12), and tends to zero as the bond half length tends to infinity.

The gain of a *uts* joint as compared to a more conventional type can be defined as the ratio of the maximum torsional moments that can be withstood by the *uts* and conventional joints, once a certain collapse phenomenon has been assumed. If we suppose that joint collapse takes place when the maximum predominant field stress (Eq. (11)) -a estimate of the Von Mises equivalent stress [32,35]- is equal to an ultimate value σ_u characteristic of the adhesive, the foregoing relations show how the *uts* joint's gain over the conventional type coincides with its stress peak parameter (Eq. (13)):

$$M_u:\sigma_{y_{\max}}=\sigma_u, \quad \frac{M_{\substack{u\\uts}}}{M_{\substack{u\\single-lap\\scarf}}}\equiv\lambda_{\substack{single-lap\\scarf}} \tag{14}$$

This means that for a particular type of joint, the ratio of the maximum torsional moment that can be transmitted by the *uts* joint and by the joint in question coincides exactly with the ratio of the maximum stress to the mean stress on the critical joint plane ($z= b/2$).

The optimised joint is thus both lighter and stronger as regards the type of collapse assumed.

However, it is important to note that adhesive bonded joints, non-tubular ones in particular, are by nature susceptible to brittle collapse. If the full benefits of the *uts* joint geometry are to be enjoyed, it is thus essential that appropriate technological measures be introduced to ensure that joint collapse cannot involve mechanical fracture phenomena.

Conclusions

The paper addresses the problem of optimising a non-tubular adhesive bonded joint for torsion, a type of characteristic of internal reaction to which the non-tubular joint is quite sensitive.

The presence of stress peaks at the ends of the bond area for *single-lap* joints, and at the centerline for *scarf* joints suggested that an optimised intermediate profile could be found.

Through appropriate design of the bonded beam profiles, it was possible to level the stress field and thus produce joints with uniform torsional strength. The stress field in the adhesive of the optimised joint is constant along the length, and thus has no stress peaks.

This result is of considerable practical utility and, once brittle failure of the joint has been ruled out technologically, makes it possible to produce adhesive bonded joints which are both lighter and stronger under torsion.

Acknowledgements

The author would like to thank Prof. G. Surace, Prof A. Carpinteri, Dr. C. Surace and the Italian National Research Council and the Fiat Research Centre for funding this work.

References

1 Adams, R.D. and Peppiatt, N.A. (1977) Stress analysis of adhesive bonded tubular lap joints. *J. Adhesion,* 9, 1-18.
2 Alwar, R.S. and Nagaraja, Y.R. (1976) Viscoelastic analysis of an adhesive tubular joint. *J. Adhesion*, 8, 79-92.
3 Bryant, R.W. and Dukes, W.A. (1965) The measurement of the shear strenght of adhesive joints in torsion. *Brit. J. Appl. Phys*., 16, 101-108.
4 Chen, D. and Cheng, S. (1992) Torsional stress in tubular lap joints. *Int. J. Solids and Structures,* 29, 845-853.
5 Chen, D. and Cheng, S. (1992) Torsional stresses in tubular lap joints with tapered adherends. *J. Engineering Mechanics-ASCE,* 118, 1962-1973.
6 Choi, J.H. and Lee, D.G. (1994) The torque transmission capabilities of the adhesively-bonded tubular single lap joint and the double lap joint. *J. Adhesion,* 44, 197-212.
7 Chon, C.T. (1982) Analysis of tubular lap joint in torsion. *J. Composite Materials*, 16, 268-284.
8 Gent, A.N. and Yeoh, O.H. (1982) Failure loads for model adhesive joints subjected to tension, compression or torsion. *J. Materials Science,* 17, 1713-1722.
9 Graves, S.R. and Adams, D.F. (1981) Analysis of a bonded joint in a composite tube subjected to torsion. *J. Composite Materials*, 15, 211-224.
10 Hipol, P.J. (1984) Analysis and optimisation of a tubular lap joint subjected to torsion. *J. Composite Materials*, 18, 298-311.
11 Jeong, K.S., Lee, D.G., Kwak, Y.K. (1995) Application of adhesive joining technology for manufacturing of the composite flexspline for a harmonic drive. *J. Adhesion,* 48, 195.

12 Kim, K.S., Kim, W.T., Lee, D.G., Jun, E.J. (1992) Optimal tubular adhesive-bonded lap joint of the carbon-fiber epoxy composite shaft. *Composite Structures,* 21, 163-176.
13 Kim, W.T. and Lee, D.G. (1995) Torque transmission capabilities of adhesively bonded tubular lap joints for composite drive shafts. *Composite Structures,* 30, 229-240.
14 Lee, D.G., Kim, K.S., Im, Y.T. (1991) An experimental-study of fatigue-strength for adhesively bonded tubular single lap joints. *J. Adhesion,* 35, 39-53.
15 Lee, S.J. and Lee, D.G. (1992) Development of a failure model for the adhesively bonded tubular single lap joint. *J. Adhesion,* 40, 1-14.
16 Lee, S.J. and Lee, D.G. (1995) An iterative solution for the torque transmission capability of adhesively-bonded tubular single lap joints with nonlinear shear properties. *J. Adhesion,* 53, 217-227.
17 Lee, S.W., Lee, D.G., Jeong, K.S. (1997) Static and dynamic torque characteristics of composite cocured single lap joint. *J. Composite Materials*, 31, 2188-2201.
18 Lubkin, J.L. and Reissner, E. (1956) Stress distribution and design data for adhesive lap joints between circular tubes. *Trans. ASME*, 78, 1213-1221.
19 Matsui, K. (1991) Size effects on nominal ultimate shear stresses of adhesive-bonded circular or rectangular joints under torsion. *Int. J. Adhesion and Adhesives,* 11, 59-64.
20 Matsui, K., Ueda, Y., Aihara, Y., Miyazaki, H. (1986) Size-effect on ultimate shear stress of adhesive-bonded tubular lap or tubular butt or circular scarf butt joint under twisting load. *J. Adhesion Soc. Japan*, 22, 479-483.
21 Matsui, K., Ueda, Y., Morikawa, Y., Yoshino, T. (1987) Size-effect on ultimate torsional stress of adhesive-bonded joint with a rectangular cross section. *J. Adhesion Soc. Japan*, 23, 96-102.
22 Medri, G. (1977) Il calcolo delle tensioni nell'adesivo in giunti tra tubi sollecitati da momento torcente. *Ingegneria Meccanica*, 7/8, 247-251.
23 Medri, G. (1988) Viscoelastic analysis of adhesive bonded lap joints between tubes under torsion. *J. of vibration acoustics stress and reliability in design-transactions of the ASME,* 110, 384-388.
24 Moloney, A.C., Kausch, H.H., Stieger, H.R. (1984) The use of the double torsion test geometry to study the fracture of adhesive joints. *J. Materials Science letters*, 3, 776-778.
25 Nayebhashemi, H., Rossettos, J.N., Melo, A.P. (1997) Multiaxial fatigue life evaluation of tubular adhesively bonded joints. *Int. J. Adhesion and Adhesives*, 17, 55-63.
26 Prakash, V., Chen, C.M., Engelhard, A., Powell, G. (1995) Torsional fatigue test for adhesive-bonded butt joints. *J. Testing and Evaluation,* 23, 228-230.
27 Pugno, N. and Surace, G. (1998) Ottimizzazione di un giunto incollato tubular-lap progettato ad uniforme resistenza a torsione*, XXVII AIAS*, 1043-1052, Perugia, Italy.
28 Rao, M.D. and Zhou, H. (1994) Vibration and damping of a bonded tubular lap joint. *J. Sound and Vibration,* 178, 577-590.
29 Reedy, E.D. and Guess, T.R. (1993) Composite-to-metal tubular lap joints strength and fatigue resistance. *Int. J. Fracture,* 63, 351-367.
30 Vonesebeck, G., Kising, M., Neuhof, U., (1996) Investigation on ceramic-metal joints for shaft-hub connections in gas-turbines. *J. of engineering for gas turbines and power-transactions of the ASME,* 118, 626-631.
31 Zhou, H.M. and Rao, M.D. (1993) Viscoelastic analysis of bonded tubular joints under torsion. *Int. J. Solids and Structures,* 30, 2199-2211.
32 Pugno, N. (1998) La torsione delle giunzioni incollate non tubolari, *Ph.D. Thesis*, Dept. of Structural Engineering, Politecnico di Torino, Torino, Italy.
33 Pugno, N. and Surace, G. (1998) Theoretical tensional analysis of a single lap bonded joint subjected to torsion*, VII NMCM*, 189-195, Hihg Tatras, Slovak Republic.
34 Pugno, N. and Surace, G. (1998) Analisi teorica tensionale di un giunto incollato double-lap soggetto a torsione*, XXVII AIAS*, 1053-1062, Perugia, Italy.
35 Pugno, N. and Surace, G. (1999) Non tubular bonded joint under torsion: Theory and numerical validation. Submitted to *Structural engineering and mechanics*.